

Field-induced first-order to second-order magnetic phase transition in $\text{Sm}_{0.52}\text{Sr}_{0.48}\text{MnO}_3$ P. Sarkar,^{1,2} P. Mandal,² A. K. Bera,³ S. M. Yusuf,³ L. S. Sharath Chandra,⁴ and V. Ganesan⁴¹*Department of Physics, Serampore College, Serampore 712 201, India*²*Saha Institute of Nuclear Physics, 1/AF Bidhannagar, Calcutta 700 064, India*³*Solid State Physics Division, Bhabha Atomic Research Center, Mumbai 400 085, India*⁴*UGC-DAE Consortium for Scientific Research, University Campus, Khandwa Road, Indore 452 017, India*

(Received 20 May 2008; published 29 July 2008)

We report on the magnetic field (H) dependence of the order of the ferromagnetic (FM) to paramagnetic (PM) phase transition in $\text{Sm}_{0.52}\text{Sr}_{0.48}\text{MnO}_3$ single crystal. For $H < 4$ T, magnetization and specific-heat data show a first-order phase transition, with sharp drop of magnetization along with hysteresis, and large, symmetric, and narrow specific-heat peak with finite amount of entropy change at T_C . By contrast, for $H \geq 4$ T, the phase transition becomes essentially second-order with tricritical point exponents $\beta \sim 0.32$ and $\gamma \sim 1.31$. The tricritical point separates first-order ($H < 4$ T) from second-order ($H \geq 4$ T) transition.

DOI: [10.1103/PhysRevB.78.012415](https://doi.org/10.1103/PhysRevB.78.012415)

PACS number(s): 75.47.Lx, 75.40.Cx

Mixed-valence manganites $R_{1-x}A_x\text{MnO}_3$ (R : rare-earth ions, A : alkaline-earth ions) exhibit a rich variety of exotic phenomena due to the presence of several competitive interactions of comparable strength. Recently, there is a considerable experimental and theoretical interest on the effect of quenched disorder on the phase transition and the appearance of colossal magnetoresistance.¹⁻⁴ Similar to antiferromagnetic and Jahn-Teller coupling, disorder also reduces the carrier mobility and the formation energy for lattice polarons and, thus truncating the ferromagnetic phase and changes the nature of the transition. The effect of disorder on the physical properties is strong when the bandwidth of the system is small. The bandwidth can be controlled by tuning the average ionic radius $\langle r_A \rangle$ of R and A ions. On the other hand, the quenched disorder arises mainly due to the size mismatch between R and A ions and its value is identified as the A -site size variance $\sigma^2 = \langle r_A^2 \rangle - \langle r_A \rangle^2$.⁵ Thus, the disorder will be large in a system with the rare-earth element of smaller ionic radius such as Sm, Eu, and Gd and alkaline-earth element of larger ionic radius such as Sr and Ba. Among these kinds of systems, $\text{Sm}_{1-x}\text{Sr}_x\text{MnO}_3$ close to $x=0.5$ shows a very sharp drop in magnetization at ferromagnetic (FM) to paramagnetic (PM) transition, where resistivity changes several decades.^{2,6,7} This suggests that FM phase is truncated, rendering the transition first order. The nature of magnetic transition has been reported on several manganites where the effect of quenched disorder is negligible.⁸⁻¹¹ However, there is no systematic analysis on the nature of magnetic phase transition in a system with large quenched disorder either in the ambient condition or in the presence of any external perturbation.

In this Brief Report, we present the detailed analysis of magnetic field (H) dependence of the order of FM-PM phase transition in $\text{Sm}_{1-x}\text{Sr}_x\text{MnO}_3$ with $x=0.48$. The reason why we have chosen $x=0.48$ is that near the half doping ($x=0.5$), the phase competition and the resultant phase variation are most clearly seen and also disorder is maximum at $x=0.5$. In particular, we have shown from magnetization, specific heat, and thermopower studies that below a critical value of applied magnetic field ($H \sim 4$ T), FM to PM transition is first order in nature and it crosses over to conven-

tional second order above that field. To the best of our knowledge, this is the first experimental analysis on the change of the order of magnetic phase transition with external parameter.

Single crystals of $\text{Sm}_{0.52}\text{Sr}_{0.48}\text{MnO}_3$ were grown by using an optical floating zone furnace.¹² The quality of the crystal was carefully checked by various techniques such as electron dispersive x-ray analysis, x-ray diffraction, ac susceptibility, etc. Magnetic measurements were done using a SQUID magnetometer (Quantum Design) in fields up to 7 T and in a vibrating sample magnetometer (Oxford Instruments) up to 11.5 T using five-scan averaging. The data were collected at 1–4 K interval after stabilizing the temperature for about 45 min. External magnetic field was applied along the longest sample direction and data were corrected for the demagnetization effect. Specific-heat measurements were performed using semiadiabatic and relaxation techniques in a wide range of temperature (5–300 K) and magnetic field (0–10 T). Thermoelectric power measurements were carried out by a differential technique on the same specimen.

Figure 1(a) shows a series of isotherms of magnetization $M(H)$ (with increasing field) of $\text{Sm}_{0.52}\text{Sr}_{0.48}\text{MnO}_3$ single crystal for some selected temperatures. A large hysteresis between increasing and decreasing fields is observed. The width of the hysteresis decreases with increasing T , and it vanishes above 160 K [Fig. 1(b)]. In contrast to a continuous FM-PM transition, a field-induced steplike jump in M is clearly observed from these plots. With increasing T , the sharpness of the jump decreases and no such jump exists above 160 K. Earlier studies established that the presence of quenched disorder leads to the creation of an inhomogeneous metastable state and subsequent magnetization jumps.⁶ Often, such a field-induced steplike jump in M along with hysteresis is the indication of first-order FM transition such as in MnAs.¹³ Thus, it is important to analyze the nature of the magnetic phase transition in the ambient condition as well as in the presence of an external magnetic field. One approach is to examine the slope of Arrott plots (H/M vs M^2).¹⁴ These plots will reveal a set of parallel curves with a positive slope for the second-order transition. Therefore, the observed negative slope in low-field region (except the initial part) and positive slope in the high-field regime, where H/M vs M^2 at

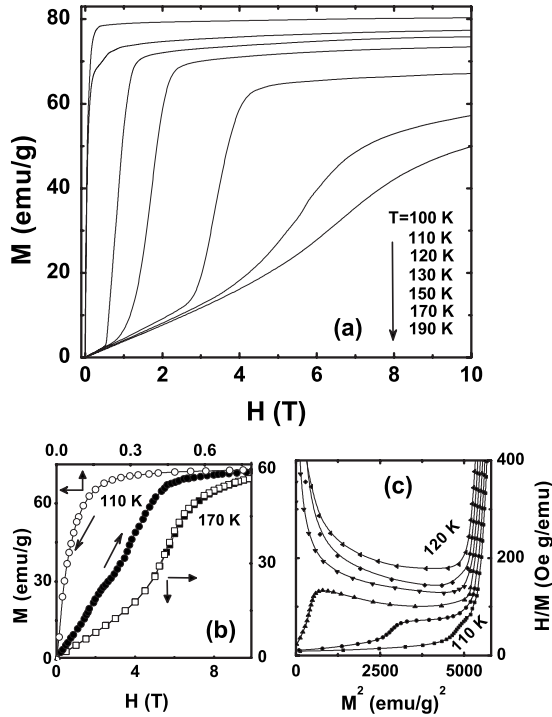


FIG. 1. (a) Isothermal magnetization (M vs H) of $\text{Sm}_{0.52}\text{Sr}_{0.48}\text{MnO}_3$ single crystal (data with increasing field are shown). (b) Hysteresis in $M(H)$ at 110 and 170 K. (c) Magnetization isotherms replotted as H/M vs M^2 between 110 K (bottom) and 120 K (top) in 2 K interval.

various temperatures tends to form a progression of parallel curves indicate that the transition is second order only at high fields [Fig. 1(c)]. According to the Banerjee¹⁵ criterion, the slope H/M vs M^2 is negative for first-order transition. This criterion has been used extensively in manganites and other systems to distinguish first-order magnetic transition from second-order ones.^{8,16} So, our results indicate that FM-PM transition in $\text{Sm}_{0.52}\text{Sr}_{0.48}\text{MnO}_3$ is first order at low fields and becomes continuous in the high-field regime.

To establish the field-induced first-order to second-order transition, we have analyzed T dependence of M for different H [Fig. 2(a)]. It is clear that the ferromagnetic transition is notably sharp for small H and the sharpness decreases at high fields. To describe the change quantitatively, we have calculated the peak width at half maximum (Δ_M) of dM/dT vs T curve for different H . Δ_M is small and almost independent of H below 4 T, but increases sharply above this field [Fig. 2(b)]. This kind of dependence of Δ_M on H indicates that 4 T is a critical field around which the nature of the magnetic phase-transition changes.¹⁷ One can see that the application of magnetic field shifts the transition temperature, and thus leads to a field-dependent phase boundary T_C vs H [Fig. 2(c)]. The phase diagram shows two critical end points for $H < 4$ T [determined from the thermal hysteresis of M as shown in the inset of Fig. 2(b)] and one end point above 4 T. The width of the thermal hysteresis at $H \sim 0$ is about 4 K, which narrows progressively with increasing field and disappears above 4 T. Thus, the two phase-transition lines AC and BC converge into a single phase-transition line above 4 T. This confirms that the system has a tricritical

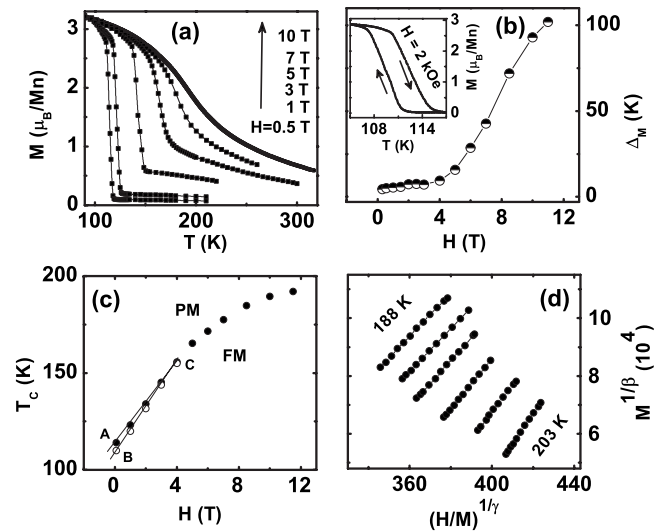


FIG. 2. (a) Temperature dependence of magnetization (heating cycle) for $\text{Sm}_{0.52}\text{Sr}_{0.48}\text{MnO}_3$ single crystal at different magnetic fields. (b) H dependence of Δ_M . Inset shows thermal hysteresis of M at $H=2$ kOe. (c) T_C - H phase diagram. Closed and open symbols are transition temperatures derived from the heating and cooling cycles of $M(T)$ curves, respectively. (d) Modified Arrott plots $[M^{1/\beta}$ vs $(H/M)^{1/\gamma}]$ in the high field $H \geq 9$ T and high temperature $188 \text{ K} \leq T \leq 203 \text{ K}$ (with 3 K interval) regime with $\beta=0.32$ and $\gamma=1.31$.

point ($H=4$ T), which sets a boundary between first-order ($H < 4$ T, where hysteresis exists) and second-order ($H > 4$ T, where hysteresis disappears) ferromagnetic transitions.¹⁸ It may be noted that at $H \sim 4$ T, both thermal energy associated with the width of hysteresis and the magnetic energy are comparable in magnitude. We use Clausius-Clapeyron equation to estimate the magnetic entropy change (ΔS_{mag}) of the system at $T_C=110$ K. In such a case, the Clausius-Clapeyron relation takes the form $\Delta S_{\text{mag}} = \Delta M / (dT_C/dH)$.⁹ For this purpose, we take $dT_C/dH = 11.3 \text{ K/T}$ from the linear part of Fig. 2(c) and $\Delta M = M_{\text{FM}} - M_{\text{PM}}$ is calculated from $M(H)$ curve [Fig. 1(a)]. This system exhibits a finite amount of entropy change (1.45 J/mol K) at $T_C=110$ K. To support that the phase transition becomes second order at high fields, we have replotted $M(H)$ data into a modified Arrott plot $M^{1/\beta}$ vs $(H/M)^{1/\gamma}$ [Fig. 2(d)] at high field ($H \geq 9 \text{ T}$) and high-temperature ($T \geq 188 \text{ K}$) region where H dependence of T_C is weak. In this domain of temperature and field, we observe that $M^{1/\beta}$ vs $(H/M)^{1/\gamma}$ generates almost parallel straight lines with critical exponents, $\beta \sim 0.32$ and $\gamma \sim 1.31$ as expected for a second-order phase transition.^{10,11} Taking into account the weak dependence of T_C on H in the high field and high-temperature region, we found that $T_C M^{1/\beta}$ vs $T_C [1 + (H/M)^{1/\gamma}]$ curves shows a set of parallel lines, but over a wider range of T and H without a significant change in β and γ .¹⁹

Due to the coexistence of several phases in manganites, it is difficult to analyze the nature of phase transition from magnetic measurement only.²⁰ In order to confirm the nature of the magnetic phase transition, we have measured the temperature dependence of specific heat (C_p) of

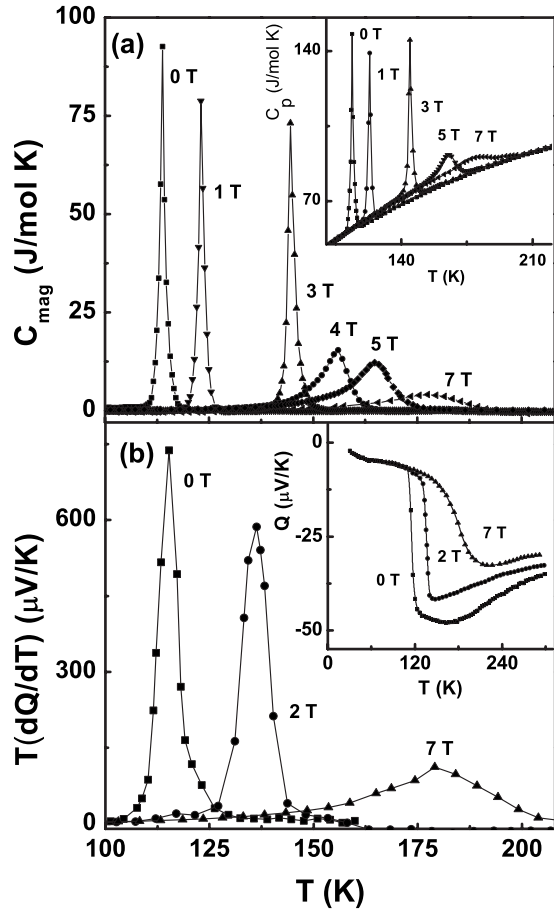


FIG. 3. (a) Molar specific heat (after subtracting the background), C_{mag} vs temperature. Inset: T dependence of specific heat (C_p) of $\text{Sm}_{0.52}\text{Sr}_{0.48}\text{MnO}_3$ single crystal for different H . (b) Thermal distribution of $T(dQ/dT)$ for different fields. Inset: T dependence of thermoelectric power (Q) of $\text{Sm}_{0.52}\text{Sr}_{0.48}\text{MnO}_3$ single crystal.

$\text{Sm}_{0.52}\text{Sr}_{0.48}\text{MnO}_3$ single crystal for different magnetic fields [inset of Fig. 3(a)]. C_p exhibits strong anomaly near T_C both in the presence and absence of magnetic field. To estimate the magnetic contribution in C_p , C_{mag} , a polynomial fit from 40 to 300 K [excluding the region $(T_C - 30) \leq T \leq (T_C + 30)$] was subtracted.²¹ Figure 3(a) shows the thermal distribution of C_{mag} for different magnetic fields. For $H=0$, C_{mag} shows a large, narrow, and symmetric peak at T_C . With increasing H , the sharpness of the peak remains almost unaltered for $H < 4$ T, but above that the sharpness decreases and the peak becomes λ -like. The shape and field dependence of C_{mag} indicate that $H \approx 4$ T is the boundary between the region where the magnetic transition is first order ($H < 4$ T) and the region where the transition is second order in nature ($H \geq 4$ T). Additionally, we have measured the temperature dependence of thermopower (Q) for different magnetic fields [inset of Fig. 3(b)]. It is clear from the figure that $Q(T)$ mimics the T dependence of M . At $H=0$, Q shows a sharp drop at T_C and the sharpness decreases with field as in the case of magnetization. As thermopower is directly related to the specific heat (C) of charge carriers ($C \sim TdQ/dT$), we have plotted TdQ/dT as a function of T for different H in

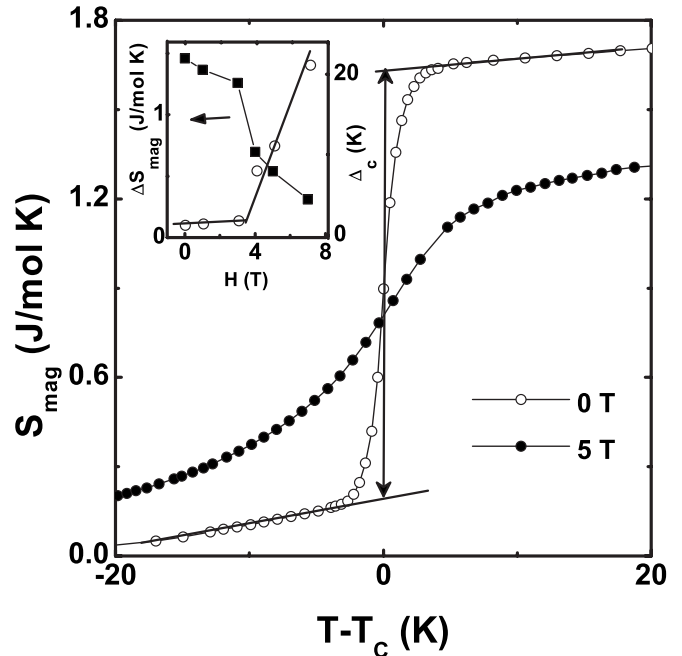


FIG. 4. Magnetic entropy S_{mag} calculated by integrating C_{mag}/T around T_C for $H=0$ and 5 T. Inset: magnetic-field dependence of ΔS_{mag} (closed square) and ΔC (open circle).

Fig. 3(b).²² The zero-field peak is sharp, narrow, and symmetric, while the peak becomes broad at $H=7$ T, qualitatively similar to C_{mag} .

The order of the magnetic phase transition can also be understood from the behavior of the entropy at the transition point. For a first-order transition one expects a discontinuous jump in entropy. For this purpose, we have calculated the magnetic entropy (S_{mag}) associated with ferromagnetic transition as $S_{\text{mag}} = \int (C_{\text{mag}}/T) dT$. In Fig. 4, S_{mag} is plotted as a function of T within a temperature interval of ± 20 K around T_C . The discontinuous and smooth changes of S_{mag} around T_C for $H=0$ and 5 T, respectively, indicate a first-order to second-order crossover of FM transition with increasing magnetic field. To describe the change quantitatively we have calculated the magnetic entropy change at T_C , ΔS_{mag} , by using the linear extrapolation of S_{mag} from below and above to T_C as depicted in Fig. 4. The value of ΔS_{mag} , calculated from magnetization and specific heat are comparable to each other. The field dependence of ΔS_{mag} and peak width at half maximum (ΔC) of C_{mag} vs T curve are shown in the inset of Fig. 4. Initially, ΔS_{mag} and ΔC do not change significantly, but at around 4 T, ΔC increases abruptly while ΔS_{mag} drops sharply. This behavior confirms that the order of FM-PM transition in $\text{Sm}_{0.52}\text{Sr}_{0.48}\text{MnO}_3$ changes from first to second order at around $H=4$ T.

It is thus clear that the magnetic phase transition in $\text{Sm}_{0.52}\text{Sr}_{0.48}\text{MnO}_3$ changes from first to second order under the influence of external magnetic field. A change from first- to second-order phase transition with the variation of external parameter is considered in Ref. 3. The theoretical model takes into account the effect of quenched disorder on the nature of the phase transition. Near the phase transition, the coherence length remains finite for a first-order transition. If

this length is sufficiently large to average out the existing inhomogeneities, the transition would be very sharp, as it should be for a first-order transition. On the other hand, if the growth of correlations is blocked by local disorder, the transition is smeared out and becomes second order in nature. The application of the external magnetic field increases the degree of magnetic inhomogeneity in the sample and thus leads to the change from first- to second-order transition with increasing field.

In conclusion, we have performed magnetization, specific heat, and thermopower measurements on $\text{Sm}_{0.52}\text{Sr}_{0.48}\text{MnO}_3$ single crystal to study the nature of the FM-PM phase transition. In the low-magnetic field regime, the data show several signatures of a first-order transition: field-induced magnetization jump, negative slope of H/M vs M^2 curves, a

discontinuous drop of magnetization (including hysteresis) and thermopower just above T_C , and sharp, symmetric, and narrow specific-heat peak with finite amount of discontinuity in entropy. All these signatures of first-order FM-PM transition disappear above a tricritical point $H \sim 4$ T and the system becomes essentially second order with tricritical point exponents $\beta \sim 0.32$ and $\gamma \sim 1.31$.

The authors would like to thank P. K. Mohanty, P. Choudhury, A. N. Das, B. Ghosh, and T. V. Ramakrishnan for enlightening discussions and A. Pal and D. Vieweg for technical assistance. Authors would also like to thank DST, India for the financial assistance for the LTHM project at CSR, Indore. L.S.S.C. would like to acknowledge CSIR, India for the Senior Research Fellowship.

¹E. Dagotto, T. Hotta, and A. Moreo, *Phys. Rep.* **344**, 1 (2001).

²Y. Tokura, *Rep. Prog. Phys.* **69**, 797 (2006).

³Y. Imry and M. Wortis, *Phys. Rev. B* **19**, 3580 (1979).

⁴M. Uehara, S. Mori, C. H. Chen, and S.-W. Cheong, *Nature (London)* **399**, 560 (1999).

⁵L. M. Rodriguez-Martinez and J. P. Attfield, *Phys. Rev. B* **54**, R15622 (1996); **63**, 024424 (2000).

⁶L. M. Fisher, A. V. Kalinov, I. F. Voloshin, N. A. Babushkina, D. I. Khomskii, Y. Zhang, and T. T. M. Palstra, *Phys. Rev. B* **70**, 212411 (2004).

⁷Y. Endoh, H. Hiraka, Y. Tomioka, Y. Tokura, N. Nagaosa, and T. Fujiwara, *Phys. Rev. Lett.* **94**, 017206 (2005).

⁸J. E. Gordon, C. Marcenat, J. P. Franck, I. Isaac, G. Zhang, R. Lortz, C. Meingast, F. Bouquet, R. A. Fisher, and N. E. Phillips, *Phys. Rev. B* **65**, 024441 (2001); J. Mira, J. Rivas, F. Rivadulla, C. Vazquez-Vazquez, and M. A. Lopez-Quintela, *ibid.* **60**, 2998 (1999).

⁹D. Kim, B. Revaz, B. L. Zink, F. Hellman, J. J. Rhyne, and J. F. Mitchell, *Phys. Rev. Lett.* **89**, 227202 (2002).

¹⁰S. Rößler, U. K. Rößler, K. Nenkov, D. Eckert, S. M. Yusuf, K. Dörr, and K.-H. Müller, *Phys. Rev. B* **70**, 104417 (2004).

¹¹K. Ghosh, C. J. Lobb, R. L. Greene, S. G. Karabashev, D. A. Shulyatev, A. A. Arsenov, and Y. Mukovskii, *Phys. Rev. Lett.*

81, 4740 (1998).

¹²P. Mandal, B. Bandyopadhyay, and B. Ghosh, *Phys. Rev. B* **64**, 180405(R) (2001); P. Mandal and B. Ghosh, *ibid.* **68**, 014422 (2003).

¹³C. P. Bean and D. S. Rodbell, *Phys. Rev.* **126**, 104 (1962).

¹⁴A. Arrott and John E. Noakes, *Phys. Rev. Lett.* **19**, 786 (1967).

¹⁵B. K. Banerjee, *Phys. Lett.* **12**, 16 (1964).

¹⁶X. Zhou, W. Li, H. P. Kunkel, and G. Williams, *Phys. Rev. B* **73**, 012412 (2006).

¹⁷R. I. Zainullina, N. G. Bebenin, V. V. Ustinov, Y. M. Mukovskii, and D. A. Shulyatev, *Phys. Rev. B* **76**, 014408 (2007).

¹⁸S. W. Biernacki, *Phys. Rev. B* **68**, 174417 (2003).

¹⁹The Arrott-Noakes equation $(H/M)^{1/\gamma} = (T - T_C)/T_C + (M/M_0)^{1/\beta}$ can be rewritten as $T_C[1 + (H/M)^{1/\gamma}] = T + T_C + (M/M_0)^{1/\beta}$. Thus $T_C M^{1/\beta}$ vs $T_C[1 + (H/M)^{1/\gamma}]$ plots will be linear and parallel to each other for different T even when T_C depends on H .

²⁰M. M. Savosta, P. Novak, Z. Jirak, J. Hejtmanek, and M. Marysko, *Phys. Rev. Lett.* **79**, 4278 (1997).

²¹J. A. Souza, Y. K. Yu, J. J. Neumeier, H. Terashita, and R. F. Jardim, *Phys. Rev. Lett.* **94**, 207209 (2005).

²²S. H. Tang, P. P. Craig, and T. A. Kitchens, *Phys. Rev. Lett.* **27**, 593 (1971).